Pilot Support for Flying Curved Decelerating Approaches in Realistic Wind Conditions

Alexander in t Veld, Rob Groenouwe, Max Mulder and René van Paassen
Faculty of Aerospace Engineering
Delft University of Technology
Delft, The Netherlands
a.c.intveld@tudelft.nl

***Abstract*—The most promising aircraft noise abatement approach procedures are those that combine flying longer at high altitude with continuous descents in a near-idle thrust setting. Although very effective at mitigating noise impact on the populated areas that surround airports, these procedures reduce runway capacity with respect to standard ILS approaches. Large uncertainties in descent trajectories force air traffic controllers to apply large separations in order to ensure safe operation. In this paper, a solution is presented that addresses the problems of variability in deceleration profiles and wind uncertainty. Spacing is done by providing pilots with a required time of arrival. A support system then helps the pilot in meeting this time goal. A wind prediction algorithm has been developed that creates a wind profile estimate along the intended three dimensional approach track, using filtered wind data observations broadcast by nearby aircrat. By combining accurate wind estimates with a flap scheduling algorithm, accurate track and speed guidance is available on-board. An interface has been designed that aids the pilot both in flying a controlled continuous descent approach and in meeting the time target set by air traffic control. To test the combined support system, a piloted simulator experiment was set up. Performance in terms of time goals was found to be consistent under all tested conditions and significantly better in comparison with the non-supported condition. Also, workload is significantly lower with the display optimization present. Providing the pilot with continuously updated time performance information based on actual meteorological circumstances was shown to be an important requirement for the implementation of CDAs in a time based spacing environment.**

***Index Terms*—continuous decent approach, wind prediction, trajectory prediction, pilot guidance**

I. Introduction

All over the western world, and especially in Europe, aircraft noise is one of the major limiting factors of airport capacity growth[1]. A lot of attention is paid to mitigating airport nuisance from the surrounding communities. Many different approaches are taken, for instance in the fields of aircraft engine technology and airport infrastructure planning[2]. The approach under study here will focus on noise abatement approach procedures, and how these can attribute to lowering aircraft noise impact on the ground. In this field there is still significant room for improvement, since the procedures currently in place hardly make use of advances in guidance, navigation and surveillance technology.

Over the years, several noise abatement approach procedures have been developed[3], [4]. Variants include general procedures like the Low-Power Low-Drag Approach or the Continuous Descent Approach, and airport-specific measures[5], [6], [7], [8]. One characteristic aspect of many of these proposed procedures is that part of the approach is carried out with more or less idle thrust settings. Also, aircraft should avoid flying level segments at low altitude, which are typical for the current standard procedures, including ILS approaches. These new procedures have been shown to reduce aircraft noise, but at a cost: the different continuous descent profiles of various aircraft cause air traffic controllers to apply large initial separations to ensure safe operation. As a result, runway capacity is reduced[6], [9].

In this paper a solution to this problem is proposed by introducing a pilot support system that enables time-based separation during the approach. In other words, pilots are given a Required Time of Arrival (RTA), rather than radar vectors. It then becomes the pilot's task to comply, within bounds, with this time goal, whereas final responsibility for safe separation remains with ATC. The resulting system enables continuous descents, while still guaranteeing safe separation. This research focuses in particular on curved approach procedures under realistic wind conditions. Wind has a major influence on the accuracy of time based separation, and prediction of the wind profile encountered during the approach could be of great importance. A tool capable of accurately predicting wind conditions along a three-dimensional approach track was developed. Together with an algorithm that calculates the optimum settings for parameters such as the altitude where thrust is reduced to flight idle, this forms a support system that helps the pilot in flying idle thrust, continuous descent approaches while meeting arrival times commanded by ATC. This should allow ATC to sequence and space aircraft in the TMA more tightly, eliminating the capacity reduction currently associated with many noise abatement procedures.

This paper discusses (i) the characteristics of the particular Continuous Descent Approach procedure investigated in this paper, (ii) the algorithms that form the pilot support system and (iii) the results of a piloted simulator experiment that was set up to test the behavior of the system under realistic circumstances.

ISBN: 978-0-615-20720-9

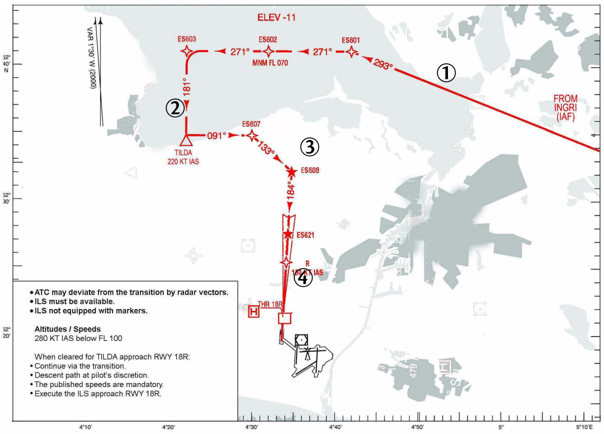

Fig. 1. The approach route, top view. The starting points of the phases of the CDA procedure are indicated. ① Level flight at FL70, ② Constant IAS descent along 3° glide path, ③ Idle thrust descent, ④ Constant final approach speed along ILS.

II. Continuous Descent Approaches

A. Description of the procedure

Based on practical experience with Noise Abatement Procedures at Amsterdam Airport Schiphol in the Netherlands and previous research[9], [6], a procedure resembling a standard nighttime transition[10] was chosen as the scenario for this research. These transitions typically involve a number of turns to avoid flying directly over the most densely populated areas. Obviously, these turns will cause great variation of the headwind and crosswind components when flying these transitions.

As can be seen from Fig. 1, the procedure consists of four parts. In phase ①, the aircraft is flying level at a relatively high altitude, but within TMA boundaries, for instance FL70. Nominal airspeed in this part is 220 kts IAS. At about 22 nm out, the aircraft intercepts a 3° glide path, but maintains its nominal indicated airspeed (phase ②). At a predetermined altitude, thrust is reduced to flight idle, marking the beginning of phase ③. When the aircraft reaches its final approach speed, thrust is reapplied and this speed is maintained (phase ④) until touchdown on the runway. For safety reasons, the aircraft should reach this approach speed no later than when it reaches 1000 ft altitude, approximately 3 nm from the runway threshold. This point will be later in this paper referred to as the reference window and is located at RNAV waypoint R (*'Romeo'*). At this point, the aircraft should be fully configured for landing, with full flaps extended and landing gear down. From here, the remainder of the approach is identical to a standard ILS approach procedure.

This type of approach procedure requires certain technologies to be available in aircraft throughout the arrival stream. For example, following a 3° glide path, while not yet aligned with the runway centerline, would require VNAV-path or Microwave Landing System (MLS) capabilities on board of the aircraft. Although not yet widely implemented, these technologies are already available today.

B. Time based separation

Variations in the characteristics of this approach trajectory would make it difficult for an air traffic controller to space incoming traffic. Three factors are identified as having an important influence on the CDA's characteristics[11]:

- Different aircraft types with their own characteristic idle-thrust deceleration profiles,
- Varying wind conditions,
- Uncertainties in pilot behavior.

As all of these factors need to be accounted for in spacing, uncertainty adds up and controllers apply large initial separations as a safety buffer. Transferring all or part of the spacing task to the cockpit could greatly reduce the problem of the different deceleration profiles, since in general the flight crew will have access to more aircraft-specific and situation-specific information on own aircraft characteristics than an air traffic controller on the ground[12]. One way to go about this is the concept of time-based separation, providing each pilot in the chain with a Required Time of Arrival (RTA) at touchdown and other waypoints along the approach trajectory. These RTAs allow the controllers to increase runway landing capacity, by providing the aircraft under their control with optimized arrival times. It then becomes the pilot's task to navigate his aircraft to the runway, respecting the time constraints as demanded by ATC. The focus of this research is to investigate whether implementation of a system of time-based separation is feasible under actual operating conditions (curved trajectories, varying winds), without putting too much workload on the flight crew.

III. Support System Design

To help the flight crew in meeting the goals stated above, a support system has been developed. Its main aim is to provide the pilot with continuous information on the aircraft's status with respect to the time goal and the execution of the continuous descent approach. The support system consists of four modules, shown as encircled blocks in Figure 2. In this section the first three modules (wind prediction (①), track prediction (②) and an optimization module (③)) are explained. The last module (module ④) translates some of the parameters in the system into information for the pilot, which is then presented on the cockpit displays, along with time performance indication. This is described in Section V.

A. Wind profile prediction

As listed in Section II-B, the wind encountered during the approach is expected to have a large influence on the accuracy with which the entire procedure is flown. It is, therefore, very important to have a tool that accurately predicts the wind profile ahead of the own aircraft. An algorithm was developed, capable of predicting horizontal wind speed and direction along any path in a three dimensional space. This wind profile prediction algorithm is based on previous research [11], which assumes measurements of wind data are available, for instance

ISBN: 978-0-615-20720-9

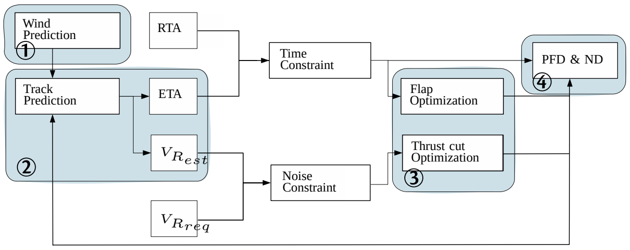

Fig. 2. Schematic of the support system algorithm. The four modules are indicated ① - ④.

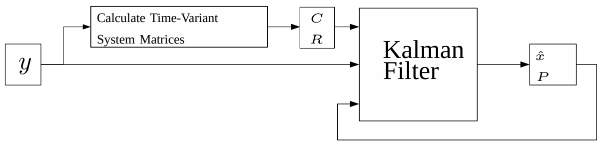

Fig. 3. Schematic of the filtering process in the wind prediction algorithm.

through ADS-B soundings from other aircraft in the vicinity. These measurements are then filtered using a Kalman filtering technique to produce an estimate of the wind profile the aircraft will encounter. The Kalman filter is well-suited to deal with integrating noisy measurements in the prediction[13]. In addition, it is easily implemented in a recursive algorithm, thereby reducing the need to store large quantities of wind data on board. This model was modified to be usable in three dimensions, making wind profile prediction along any curved approach trajectory, from any position and altitude, possible. In addition, functionality to use every incoming observation was incorporated, where in earlier work only data around certain fixed altitude intervals was used. This allows optimal use of the information at hand, and is expected to make the prediction more reliable, especially in situations where data density is low. A description of the way the wind prediction algorithm works is given below.

First, an initial wind speed estimate vector $\hat{x}$ is set up. This vector contains wind speeds for a number of altitudes. In this study, the altitude interval is set to 500 ft. This interval is arbitrary, since the accuracy of the prediction only depends on the amount and accuracy of the available wind measurements. The set up of this initial wind profile guess is arbitrary. It may consist of unfiltered measurements of ADS-B soundings, or a standard profile uploaded from an Air Traffic Services unit. In this case a standard logarithmic wind profile is constructed as follows:

$$\hat{x} = V_0 (\frac{h}{h_0})^{\kappa} \tag{1}$$

with κ the Von Karman constant, equal to 0.4[14]. This equation bases the wind speed $\hat{x}$ on the free stream wind velocity V_0 at a corresponding altitude h_0. h Is the altitude at which we want to determine the wind speed.

Whenever new data comes in, this profile is updated. An incoming observation y_k is split into North and East components, to be able to estimate these separately. Next, a weight matrix C is set up that determines the influence this observation will have on the state estimation of the wind speed. The weights in the matrix are determined based on the altitude difference between the states of interest and the measurement. With this C-matrix, the current estimate for the altitude of the observation can be calculated, and its value can be compared to the measured value to determine the innovation e. This way, an incoming measurement only influences the states in its altitude vicinity:

$$\hat{y}(k|k-1) = C(k)\hat{x}(k|k-1) \tag{2}$$

$$e(k) = y(k) - \hat{y}(k|k-1) \tag{3}$$

This innovation is multiplied with the Kalman gain to obtain a new state estimate. The Kalman gain is based on the relative magnitudes of the uncertainties in the current estimate and the new measurement, represented by the prediction error covariance matrix P and the measurement noise covariance matrix R, respectively. Since data from aircraft on the same approach track rather than elsewhere in the TMA is of more use for this prediction, the measurement noise covariance matrix R has been made dependent of the distance between the point of the measurement and the own track d:

$$R(k) = f(R_0, d(k)) \tag{4}$$

Here, R_0 represents the uncertainty in an incoming observation, mainly caused by measurement error. The accuracy of wind measurements in ADS-B soundings is approximately 2 kts[15]. The prediction error covariance matrix P is given by:

$$P(k|k-1) = AP(k-1|k-1)A^T + Q \tag{5}$$

In this equation, the matrix A represents the system dynamics. However, since the filter is used only as a noise filtering mechanism, no system dynamics are present and A reduces to the Identity matrix. Q is the (constant) process noise covariance matrix, which is determined empirically. At the same time as when the initial wind profile is set up, the P matrix is assigned a large value. This represents the large uncertainty in the accuracy of the profile at this point, and ensures that in the beginning, incoming observations have a large influence on the wind profile estimate. With this projection, the covariance of the innovation step $e(k)$ can be represented by the matrix S:

$$S(k) = C(k)P(k|k-1)C(k)^T + R(k) \tag{6}$$

The covariance matrices together determine the Kalman gain K:

$$K(k) = AP(k|k-1)C(k)^T S(k)^{-1} \tag{7}$$

A high uncertainty in the current estimate (high P) and much confidence in the accuracy of the measurement (low S)

ISBN: 978-0-615-20720-9

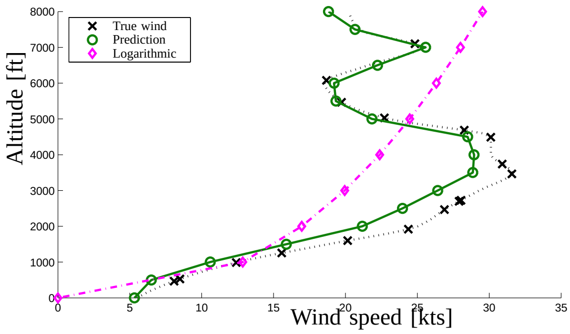

Fig. 4. Wind profile prediction performance. A typical wind profile and its estimate (in 500 ft intervals). For reference, a best-fit logarithmic profile is also shown.

yield a high value of the Kalman gain, which in turn assigns a large weight to the incoming measurement in updating the state estimate through the innovation. By the same rationale, much confidence in the current estimate and little in the accuracy of an incoming measurement yields a small value of the Kalman gain and consequently little influence of the observation on the wind speed estimate:

$$\hat{x}(k|k) = A\hat{x}(k|k-1) + K(k)e(k) \quad (8)$$

In the last step, the prediction error covariance matrix P is updated, according to:

$$P(k|k) = AP(k|k{-}1)A^T{+}Q{-}K(k)C(k)P(k|k{-}1)A^T \quad (9)$$

This iteration is repeated with a constant frequency of 1 Hz. It can be seen that when no new observation data are available, there will be no innovation, and the loop will be reduced to updating the prediction error covariance P. In this way, the uncertainty about an estimate increases when time goes by without new incoming measurements. A schematic of this loop is shown in Fig. 3.

Interpolation between the updated elements of the state vector yields the wind profile the aircraft is expected to encounter during its approach flight. The results of one such wind profile prediction are shown in Fig. 4. Here, a random wind profile (crosses) is shown, together with its best estimation (circles) based on the available observations. A best fit logarithmic profile (diamonds) is shown for reference. It becomes immediately clear that the Kalman filtering method is much more capable of capturing the random variations in realistic wind profiles. For the wind speed profiles used in the piloted simulator experiment (see Section V), the average root mean squared (RMS) of the wind speed prediction error for the Kalman filter based predictor is 2 kts, corresponding to the accuracy of the wind speed measurements available through ADS-B soundings. Prediction accuracy is much lower for a logarithmic predictor, with RMS values averaging 6 kts, occasionally running as high as 9 kts.

B. Track and time prediction

In the proposed scenario, the track to fly is fixed and determined by RNAV waypoints, as shown in Fig. 1. During the flight, an algorithm estimates the speed and time profiles along this track, taking into account the actual condition parameters such as predicted wind speed profile along this track, aircraft weight, flap setting, etc. The track prediction, consisting of speeds and times calculated for every point on the track, is repeated every second.

Between the constant speed segments of initial airspeed and final approach speed, deceleration takes place by selecting a flight idle thrust setting. This deceleration profile is influence by in varying wind conditions. Flap extension towards landing configuration also takes place in this phase, resulting in very non linear aircraft behavior. To predict the aircraft motion in this phase, a simple three degrees-of-freedom aerodynamic model of the B747-200 was used. The model is a point mass model that only looks at the forces along the flight-path and perpendicular to it. The resulting accelerations along the flight trajectory are integrated over time to yield speed, distance and time profiles. Since the model is two dimensional, it is fed with only the along-track component of the predicted wind speed.

C. Optimization of support system performance

To introduce greater flexibility and robustness in the aforementioned prediction modules, an algorithm was added to optimize two CDA parameters, flap speeds and thrust cut altitude. This third module is based on a flap scheduling algorithm, used in previous research in various forms[16], [11], [17]. It uses the same aircraft model mentioned in Section III-B, to calculate the effects of changed flap settings on the speed and time profiles in the trajectory ahead.

The flap schedule algorithm works in two modes: in HOLD mode and CAPTURE mode. In CAPTURE mode the algorithm calculates the thrust cut altitude, the altitude at which the thrust should be set to idle so that V_{APP} can be reached at h_R using the nominal flap schedule. This information is communicated to the pilot through a cue on the PFD, see Section V.

Once the thrust has been set to idle the module switches to HOLD mode. In HOLD mode the algorithm determines a flap schedule such that the aircraft reaches V_{APP} at h_R. This deviation from the nominal schedule can be used to cope with errors caused by for instance an inaccurate wind prediction, unexpected behavior from preceding aircraft, etc. In this mode, the algorithm predicts the aircrafts trajectory based on the current flap schedule. This yields an ETA, which is then compared to the RTA commanded by ATC:

$$\Delta T = ETA - RTA \quad (10)$$

Based on this difference, the flap scheduler does a rough tuning of the flaps to either their upper or their lower bounds, depending on the sign of this ΔT. In case the aircraft is predicted to arrive early, deceleration needs to be faster than the current (nominal) flap schedule will provide. The flaps

ISBN: 978-0-615-20720-9

will thus be set to their upper bounds, and the resulting new trajectory is calculated. This process is repeated for the consecutive flaps, until the target is overshot (ΔT changes sign). From here, the flap scheduler fine tunes the previous flap speed so that the aircraft arrives exactly at its RTA.

The combination of thrust cut altitude and flap selection speeds ultimately determines the CDA performance. Changes in the one parameter necessarily cause changes in the other, if the *safety goal* is not to be violated. For example, if thrust reduction is delayed (executed at a lower altitude), the aircraft will reach h_R with a speed higher than the approach speed. This can be prevented by selecting flaps at speeds higher than according to the nominal schedule, in order to increase the deceleration rate. The upper and lower bounds of the flap speeds hence define the boundaries of the control space the pilot has during the approach. Within this control space, the pilot can maneuver the aircraft to anticipate or delay his arrival time. The *time goal* requires that the aircraft touches down within a small time window around the RTA. With the aircraft on final approach, the majority of the work needed to reach this goal is already done. The flap scheduler algorithm helps the pilot to fine-tune his exact arrival time. Off-line simulations have shown that for a straight-in continuous descent approach from 7000 ft, 250 kts IAS, this control space is limited to 8-30 seconds, depending on wind conditions[11]. For this reason, it is important that the flight crew is able to steer their aircraft to within these bounds, before they start the descent.

IV. Pilot Interface

Conventional Display

In the base-line condition, the pilot interface consists of a conventional Primary Flight Display (PFD), Navigation Display (ND) and a display showing the Mode Control Panel (MCP). The required information for the time based CDA procedure is printed on two cue cards. This cueing system is loosely based on one developed at the Massachusetts Institute of Technology[18]. This system places gates at strategic locations on the track. These gates correspond to information on thrust setting, aircraft configuration and time. One cue card is designed to focus primarily on the *safety goal*, by providing the pilot with continuous descent parameter information in the final phase of the approach. The card shows a profile view of the track to fly, comparable to conventional approach charts. For four wind speeds (0, 15, 30 and 50 kts) and three wind directions (headwind and crosswind from either side on Final), the thrust cut altitude and speeds for Flaps 5, Flaps 10 and Flaps 20 are given in a table. The pilot has to interpolate between these parameters to match them with the actual situation. The printed wind speeds assume a logarithmic wind profile with the reference wind speed measured at 7000 ft altitude.

The second cue card focusses on the *time goal*, by providing the pilot with time gates at certain waypoints. The card shows a top view of the track to fly, comparable to Figure 1. The time slots at these gates are based on the aircraft following the nominal speed (IAS) profile. Taking the wind conditions

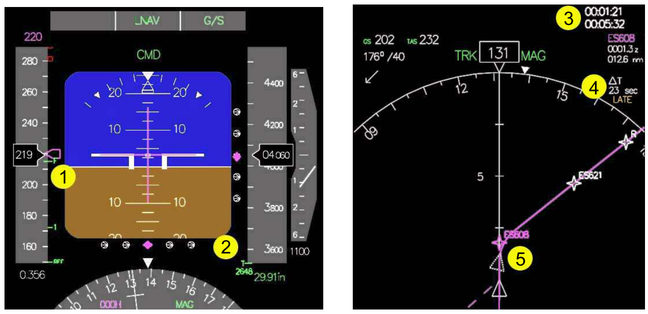

(a) Primary Flight Display (b) Navigation Display

Fig. 5. Display Modifications. (a) PFD, with ① the Flap Cue and ② the Thrust cue. (b) ND, with ③ Elapsed time and RTA, ④ Time performance and EARLY/LATE indicator and ⑤ Ghost symbol.

mentioned above (4 wind speeds, two directions) into account then yields a series of time-over-waypoint datasets. These datasets are displayed in a table.

Augmented Display

The information produced by the prediction and optimization algorithms described in Section III must be presented to the pilot in a logical and intuitive way. Display modifications and augmentations must also be designed to minimize clutter on the current lay-out of displays. The modifications explained below are shown in Figure 5.

One cue was added to help meet the *safety goal*. To indicate the altitude where thrust should be reduced to flight idle in order to meet the approach speed V_{APP} at h_R, a letter 'T' is added on the altitude tape of the Primary Flight Display. This is shown as item ② in Figure 5(a).

To help meeting the *time goal*, a series of display augmentations was introduced. To minimize ΔT in the final phase of the arrival, a letter 'F' is presented on the speed tape of the PFD at the optimal speed for the next flap selection. This is shown as item ① in Figure 5(a). On the Navigation Display, several augmentations are present. The elapsed time since the start of the approach and the Required Time of Arrival are shown as item ③ in Figure 5(b). At ④ an indication of the current situation with respect to the RTA is given as ΔT in seconds, combined with an amber EARLY/LATE indication in case this deviation is greater than 10 seconds. This time indication is also shown in a ghost symbol, through item ⑤. This ghost is an image of the own aircraft flying the intended approach track, keeping a position where the aircraft should be if ΔT were zero. The ghost symbol is a dashed variant of the white (solid line) own aircraft symbol.

V. Piloted Experiment

To test the effectiveness of time-based spacing and identify the operational constraints of implementation, a piloted experiment was conducted. Seven professional airline pilots tested the system under various operating conditions in a fixed base flight simulator.

ISBN: 978-0-615-20720-9

TABLE I
PILOT EXPERIENCE.

	Age	Aircraft types	Flying hours
Pilot A	68	DC3, CV640, DC8, B747-3/400, C550	13200
Pilot B	31	F100	1200
Pilot C	31	B747-400	300
Pilot D	23	PA28, DA42	190
Pilot E	50	military, B737, BA146, DC10, A320	12500
Pilot F	33	B757, B767	6000
Pilot G	26	B747-400	1650

Independent variables

First, two displays were defined. One, corresponding to the baseline condition, was a conventional display layout consisting of a Navigation Display (ND) and Primary Flight Display (PFD). The second display, for the augmented condition, consists of an ND and a PFD extended with information derived from the flap scheduler and optimization algorithms, as described in Section IV.

Second, four different wind conditions are defined that together represent a realistic set of wind conditions that could be encountered during any approach. A typical wind profile is shown in Figure 4. These profiles are all taken from data sets of actual wind measurements, but scaled and rotated to correspond to the wind speeds of interest. These wind conditions, listed in Table II, comprise two headwind conditions on Final, and two crosswind conditions. For each wind direction, two wind speeds at the starting altitude of 7000 ft are defined. The choice for wind speed values is such that the lower value could be encountered under normal, regularly occurring circumstances. The higher wind speed occurs in more rare situations. The wind speeds for crosswind approaches are lower, in correspondence to crosswind and headwind limits for landing.

Experiment design

The experiment design matrix is factorial, combining the four wind conditions with both displays. This yields eight experiment runs per pilot. Seven professional airline pilots (over 4500 flying hours on average, see Table I) flew a set of these eight runs, yielding 56 experiment runs in total. Each set was preceded by four to six practice runs, to familiarize the pilots with the procedure and wind conditions.

Apparatus

The experiment was conducted in the fixed base research simulator at the Control & Simulation Division. The pilots were seated on the co-pilot side, controlling the aircraft with a side stick. The Primary Flight Display, Navigation Display and the Mode Control Panel were shown on two 18" screens. An outside visual was shown of a landscape with a fictitious airport with two parallel runways.

Aircraft

The aircraft model used is a non-linear six-degrees-of-freedom model of the Boeing 747-200. The flight is executed with the autopilot in LNAV mode, leaving only manual pitch control and throttle control to the pilot. The reason for maintaining partial manual control throughout the flight was to introduce a basic level of workload during the approach. With autopilot engaged and no radio traffic or ATC present, an experiment run would comprise a lot of idle time between autopilot inputs. For guidance along a three-dimensional glide path, a Microwave Landing System (MLS)-type vertical guidance was available. This allows the pilot to fly a continuously descending path, irrespective of his position with respect to the runway. To improve lateral stability, a yaw damper was added.

TABLE II
INITIAL CONDITIONS

	Wind speed [kts]	Wind dir. [°]	Airspeed [KIAS]	Distance to go [nm]	RTA [min:sec]
A	26	90	270	47.7	11:23
B	26	180	270	46.3	11:46
C	44	180	250	31.6	09:39
D	12	90	250	30.8	07:59

Scenario

Initial conditions, such as position along the track and airspeed, are varied per wind condition, to limit the influence of learning effects on the way the track is flown. The required arrival times are tuned to each initial condition, based on a relative deviation from the nominal RTA for that condition, so that only the effects of the wind conditions influence the pilot's performance. The initial conditions are listed in Table II. In the level flight segment following each initial condition, the pilot can position the aircraft as good as possible for meeting the RTA. This is done by choosing a higher airspeed (in case a pilot is late), or a lower airspeed (in case a pilot is early) than the 220 kts chosen for the nominal speed profile. The pilot then has to maintain this airspeed until his ΔT is reduced to zero, after which he can return to the nominal 220 kts until the point of thrust cut.

Procedure

The pilot's task is to fly a Continuous Descent Approach, while meeting both *safety* and *time goals*. The aircraft starts in one of the initial conditions listed in Table II at an altitude of 7000 ft, with Flaps 1° extended and with autopilot and autothrottle engaged. The pilot is given an RTA, which is entered through an interface window in the Mode Control Panel. After this, the autopilot is switched to LNAV mode, and the autothrottle is disengaged.

Dependent measures

The dependent variables consist of both objective and subjective measures. Objective measures include operational performance and pilot control activity. Operational performance was judged by measuring the accuracy with which the targets were reached. For the *safety goal*, the deviations from the final approach speed V_{APP} at the reference window and in the remainder of the approach were measured. For the *time goal*, the deviation from the RTA was measured.

ISBN: 978-0-615-20720-9

TABLE III
DEPENDENT MEASURES

	Measure	Description
Safety goal	ΔV_{APP}	Deviation from V_{APP} at 'R'
	ΔV_{final}	RMS of the deviation from V_{APP} at 'R'
	Flap setting	Aircraft should be fully configured at 'R'
Time goal	ΔT	Deviation from the RTA at 'R'
Workload		Number of throttle setting changes
		NASA Task Load Index (TLX) score

Pilot control activity was measured by counting the number of thrust changes during a run. The subjective measures were taken from a questionnaire, aimed at giving an insight into pilot acceptance of the system, and a NASA Task Load Index (TLX)[19] sheet to assess pilot workload for each run. The dependent measures are listed in Table III.

Hypotheses

The first hypothesis is that for the augmented display time performance will improve with respect to the baseline condition. The reasoning for this is that with the help of the support system, the pilot has continuous information about his *time goal* performance at hand, which will allow for smoother and more accurate transitions between the different phases in the flight. When time information is only provided at discrete points (the gates), own performance estimation is clearly more difficult.

Secondly, CDA performance (reaching the approach speed of 150 kts at 'R', preferably no sooner but definitely not later) is expected to increase. The idea is that this performance mainly depends on the moment of thrust cut. The altitude where this is done depends heavily on the wind speed and direction on Final, so a more accurate prediction of this wind profile will increase the *safety goal* performance.

Finally, it is hypothesized that workload will be higher for the baseline condition, since in this case the pilot will have to interpolate continuously between the data on his cue cards to retrieve the appropriate parameters. Moreover, the wind used to set up the cue card data resembles standard logarithmic profiles. The discrepancy between this profile and the actual wind will require extra corrective pilot action, hence increasing the workload.

VI. RESULTS AND DISCUSSION

A. Operational Performance

Two types of performance measures are selected, each related to either the *safety goal* (mandatory performance targets) or the *time goal* (optimization). It appeared throughout the experiment that the variation in wind *speed* does not have a significant influence on performance ($F_{2,6}$ = 0.244, p = 0.784 for the *safety goal*, $F_{2,6}$ = 1.930, p = 0.156 for the *time goal*). For that reason, the four wind conditions are reduced to two clusters, defined by the wind direction.

Safety goal: To investigate how well the aircraft is established for landing at the reference window, three performance parameters are defined. The first one is the deviation from the target approach speed of 150 kts IAS, when passing the reference window (waypoint 'R', 3.14 nm from touchdown, 1000 ft altitude). The means and 95% confidence intervals for this score per wind condition (headwind or crosswind) are plotted in Figure 6(a). In this figure the deviation for the optimized configuration is lower in both headwind and crosswind, but this effect is obscured by the large spread in the data. An analysis of variance (ANOVA) shows that this spread is indeed too large to see any differences; the effect of the display configuration on the speed deviation is not significant ($F_{1,6}$ = 0.023, p = 0.883).

What can be seen from the error bar plots, is that crosswind has a negative effect on safety performance. Although most of the time hidden by the relatively large variances, this effect is significant for the deviation from V_{APP} at 'R', when the optimized display configuration is used ($F_{1,6}$ = 9.160, p = 0.023). This can be explained by the fact that the display optimization only uses the headwind component of the estimated wind speed to predict its time and speed profile. In a headwind condition, this works out well, but in a crosswind on Final, an error is introduced: the algorithm assumes a near-zero headwind component, while in reality the aircraft needs to compensate for the crosswind in order to stay on its ground track. As this is usually done by 'crabbing' the aircraft, the actual ground speed will be lower than the predicted ground speed. As a consequence, the airplane starts lagging behind the original predicted time profile, which in turn causes pilots to delay flap selection in order to maintain a higher airspeed. In many cases, the *safety goal* suffers from this decision, with the average approach speed going up from little over 151 kts to 156 kts. For the baseline condition, the data on the cue cards is based on trial runs, instead of predictor data. So, since the accuracy of the wind information on the cards (based on logarithmic profiles) is always the same, the deviation from V_{APP} is not influenced by the direction of the wind.

The fact that speed performance goes down when the track prediction is less accurate (in the crosswind condition) suggests that pilots closely followed the cues presented on the displays. At the same time, the large spread of the speed performance in the baseline condition indicates big differences in the flying strategies, adopted by each pilot. This is confirmed by the pilots' answers to a questionnaire, which showed that they used the CDA-parameter cue card mostly to determine the thrust cut altitude, but thereafter relied more on their pilot experience to determine flap selection. In the optimized display configuration, the need to look away from the instruments to check the cue cards is eliminated, and pilots use the displayed instructions.

Time goal: The main check on the time performance is the deviation from the RTA at the reference window. The means and 95% Confidence Intervals for this parameter are shown in Figure 6(b). Clearly, the average time performance is better with the aid of display optimization. An ANOVA

ISBN: 978-0-615-20720-9

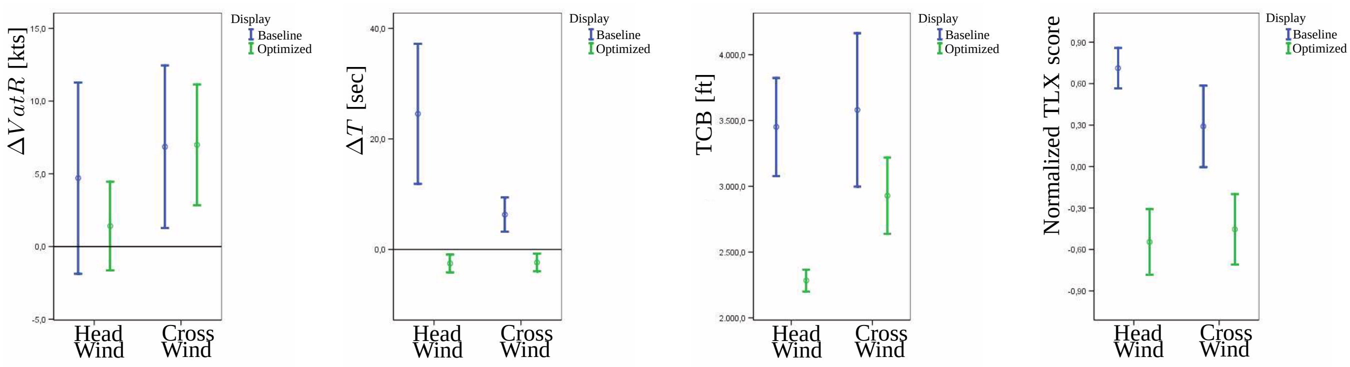

(a) The means and 95% confidence intervals for the deviation from V_{APP} at h_R.

(b) The means and 95% confidence intervals for the deviation from the RTA.

(c) The means and 95% confidence intervals for the thrust cut altitude.

(d) The means and 95% confidence intervals for the normalized NASA Task Load Index (TLX) scores.

Fig. 6. CDA performance scores.

shows that this influence is indeed significant ($F_{1,6}$ = 7.368, p = 0.033). Average time performance is within 4 seconds of the RTA. This is definitely accurate enough to guarantee safe separation. This result would allow air traffic controllers to space incoming traffic more tightly, increasing runway throughput capacity. The addition of the proposed automation to existing cockpit displays enables pilots to fly a time based CDA.

The explanation for this improvement is twofold. First, by providing the pilot with continuously updated information on his ETA status, he is able to very accurately adjust the aircraft's speed profile to minimize ΔT. In the baseline, the number of intermediate time gates is limited to four (for conditions C and D in Table II) or five (for conditions A and B). Second, the more accurate wind prediction that is available in the enhanced display condition yields a better estimate of the optimal altitude for thrust reduction. This can be seen in Figure 6(c), showing the altitude where pilots cut back on thrust to decelerate the aircraft to 150 kts. Regardless of wind direction, this altitude is significantly lower in the optimized display condition than in the baseline condition ($F_{1,6}$ = 3.560, p = 0.098). With the used wind profile class in mind (see Figure 4), it becomes clear that the logarithmic profile prediction is not able to deal with the increase in wind speed around 3500 ft. The aircraft encounters more (head)wind than expected, so its thrust cut altitude should be lowered. The track prediction and optimization routines take this effect into account.

Although the automation provided a major improvement in time performance, speed performance (deviation from V_{APP}) was still in the same range as in the baseline situation. This might be due to the fact that the the automation mainly focussed on achieving the time goal. To strike a better balance between the two performance criteria, and to provide a more logical lay out of the presented clues, it is recommended to let the cues on the Primary Flight Display focus on CDA performance (arrive stabilized at the reference window), while the cues on the Navigation Display (ghost and ΔT) focus on the time goal. Another improvement would be to integrate the cues more tightly with current procedures. For example, in many aircraft the landing gear should be lowered between two fixed consecutive flap settings. To incorporate such information in the pilot support system would ease implementation and increase acceptability by airlines and flight crew.

B. *Pilot workload*

The results for the subjective workload measurements are represented by the normalized NASA TLX rating scores in Figure 6(d). From this it becomes clear that the workload experienced by the pilots is lower for the optimized display condition, in all wind conditions. This effect is highly significant ($F_{1,6}$ = 50.390, $p < 0.001$), an observation that is confirmed by the questionnaire answers with all pilots indicating a higher workload in the baseline condition. In contrast, the workload in this type of noise abatement procedure with the optimization present was considered comparable to that of a conventional ILS approach.

Furthermore, it can be seen that for the baseline condition, the workload score also depends on the wind direction. The score is significantly lower in crosswind conditions on Final ($F_{1,6}$ = 12.797 , p = 0.012). Several factors could influence this phenomenon. First, in a headwind condition, the full force of the sharp changes in wind speed along the altitude profile is felt. In a crosswind, only one component of the wind is of influence, so the absolute change in wind speed is smaller. Another factor might be that the crosswind condition on Final means a headwind condition between waypoints TILDA and EH608 (see Figure 1). In many cases, this is the phase where pilots reach the on-time schedule ($\Delta T = 0$ and reduce speed from 250 or 270 kts to the nominal speed of 220 kts. This is not always an easy task, since a B747 in this situation (Flaps 1°, gear up, 3° glide path, no speed breaks) has a very low deceleration rate. A headwind in this situation reduces the kinematic flight path angle, which makes it easier for the pilot to decelerate the aircraft. This increases the chances of a stabilized approach and hence reduces pilot workload.

 ISBN: 978-0-615-20720-9

Flying a CDA already puts more demand on the flight crew than a regular arrival, where the basic control task is following ATC vectors. Although the tasks of flying and navigation are normally shared between the Pilot Flying and the Pilot Not Flying, the persons interviewed indicated that they would find the sharp increase in workload as experienced in the base-line scenario unacceptable.

VII. Conclusions

This paper investigated the feasibility of introducing time based spacing in realistic, three dimensional continuous descent approaches under actual wind conditions. For reasons of safety, it is important that *(1)*, the continuous descent ends in a stabilized approach configuration and speed some distance before the runway and *(2)*, pilots adhere to the required arrival times demanded by ATC, in order to maintain safe separation throughout the approach.

The development of an FMS based prediction and optimization system combined with a pilot support interface enables the flight crew to reach these two goals. A wind prediction algorithm that makes use of weather information broadcast by other aircraft in the TMA makes accurate wind profile prediction along the approach trajectory possible. Wind speed prediction error along a 30-45 nm approach trajectory is 2 kts. An accurate knowledge of the wind ahead makes sure an optimal thrust cut altitude and flap speed schedule can be selected. The piloted experiments show a strong improvement in time performance when continuously updated information on this goal is present on the display. Pilots are able to reach their RTAs within an average margin of 4 seconds, regardless of wind conditions. The average speed performance (being stabilized at a reference window) is unaffected by display optimization, although the presence of automation reduces the spread in this performance criterion. The addition of time constraints without extra aids would result in an unacceptable increase in workload, due to the continuous calculation and interpolation the pilots have to perform. Workload is significantly lower with the display optimization present, and at the same level as in current ILS approach procedures.

VIII. Recommendations

The piloted experiment shows the feasibility of time-based continuous descent approach procedures under realistic wind conditions, along a fixed trajectory. The pilot's control space to reach an RTA could be greatly enlarged by adopting a more flexible approach route. Shortening or extending the length of the track to fly, similar to the 'tromboning' technique currently used by ATC, should reduce the need for speed changes, thereby improving predictability of the speed profile during the approach.

References

[1] ICAO, "Outlook for air transport to the year 2015," International Civial Aviation Organization, 2005.

[2] ——, "Assembly resolution a33-7: Consolidated statement of continuing icao policies and practices related to environmental protection," International Civial Aviation Organization, 2001.

[3] E. H. Bolz and L. M. Reuss, "System study of advanced operational procedures for noise reduction," NASA (Task Order (TO) 56), Tech. Rep., 2001.

[4] Sourdine, "Sourdine ii, d9-1, final report," Tech. Rep., 2006.

[5] A. D. Kershaw, D. P. Rhodes, and N. A. Smith, "The influence of atc in approach noise abatement," *3rd USA/Europe Air Traffic Management R&D Seminar Napoli*, 2000.

[6] L. J. Erkelens, "Research into new noise abatement procedures for the 21st century," *AIAA GNC Conference and Exhibit, 14-17 August 2000, Denver (CO)*, 2001.

[7] J. P. B. Clarke, N. T. Ho, L. Ren, J. A. Brown, K. R. Elmer, K. O. Tong, and J. K. Wat, "Continuous descent approach: Design and flight test for louisville international airport," *Journal of Aircraft*, vol. 41, no. 5, 2004.

[8] F. Wubben and J. Busink, "Night time restrictions at amsterdam-schiphol," to70 Aviation & Environment, under Contract of the Ministry of Transport, Public Works and Water Affairs, Tech. Rep., 2004.

[9] L. Ren, J.-P. Clarke, and N. T. Ho, "Achieving low approach noise without sacrificing capacity," *22nd Digital Avionics Conference, 12-16 October 2003, Indianapolis (IN)*, 2003.

[10] Anon., "Schiphol rnav night instrument approach chart, sugol, river and artip transitions to rwy 18r," Air Traffic Control the Netherlands, Tech. Rep., 2006.

[11] W. F. de Gaay Fortman, M. M. van Paassen, M. Mulder, and A. C. in 't Veld, "Design of a pilot support system to implement time-based spacing for decelerating approaches," *AIAA GNC Conference and Exhibit, 15-18 August 2005, San Francisco (CA)*, 2005.

[12] M. F. Koeslag, "Advanced continuous descent approaches," Master's thesis, Faculty of Aerospace Engineering, Delft University of Technology, 1999.

[13] P. S. Maybeck, *Stochastic Models, Estimation and Control*. Academic Press, 1979, vol. 1.

[14] P. Frenzen and C. A. Vogel, "On the magnitude and apparent range of variation of the von karman constant in the atmospheric surface layer," *Boundary-Layer Meteorology*, vol. 72, 1995.

[15] D. Painting, "Amdar reference manual," World Meteorological Organization - AMDAR Panel, Tech. Rep., 2001.

[16] K. F. M. Schippers, J. L. de Prins, M. M. van Paassen, M. Mulder, A. C. in 't Veld, and J.-P. Clarke, "Investigation of a three-degree decelerated approach of a twin engined jet aircraft under actual flight conditions," *AIAA GNC Conference and Exhibit, 15-18 August 2005, San Francisco (CA)*, 2004.

[17] A. C. in 't Veld, M. M. van Paassen, M. Mulder, and J.-P. Clarke, "Pilot support for seperation assurance during decelerating approaches," *AIAA GNC Conference and Exhibit, 16-18 August 2004, Providence (RI)*, 2004.

[18] N. T. Ho, "Design of aircraft noise abatement approach procedures for near-term implementation," Ph.D. dissertation, Massachusetts Institute of Technology, Cambridge, MA, 2005.

[19] S. G. Hart and L. E. Staveland, "Development of nasa-tlx (task load index): Results of emperical and theoretical research," *Human Mental Workload*, pp. 239–250, 1988.

ISBN: 978-0-615-20720-9